International Journal of Engineering, Mathematical and Physical Sciences
ISSN: 2517-9934
Vol:3, No:7, 2009

Investigation of Buoyant Parameters of k-ε Turbulence Model in Gravity Stratified Flows

A. Majid Bahari, and Kourosh Hejazi

Abstract**—**Different variants for buoyancy-affected terms in k-ε turbulence model have been utilized to predict the flow parameters more accurately, and investigate applicability of alternative k-ε turbulence buoyant closures in numerical simulation of a horizontal gravity current. The additional non-isotropic turbulent stress due to buoyancy has been considered in production term, based on Algebraic Stress Model (ASM). In order to account for turbulent scalar fluxes, general gradient diffusion hypothesis has been used along with Boussinesq gradient diffusion hypothesis with a variable turbulent Schmidt number and additional empirical constant $c_{3\varepsilon}$.To simulate buoyant flow domain a 2D vertical numerical model (WISE, Width Integrated Stratified Environments), based on Reynolds-Averaged Navier-Stokes (RANS) equations, has been deployed and the model has been further developed for different k-ε turbulence closures. Results are compared against measured laboratory values of a saline gravity current to explore the efficient turbulence model.

Keywords**—**Buoyant flows, Buoyant k-ε turbulence model, Saline gravity current.

I. Introduction

GRAVITY stratified and buoyancy-affected flows are very dominant in many flow domains in different fields of engineering in hydraulics and fluid mechanics; transient stratification in estuaries and coastal zones due to salt intrusion, gravity currents in lakes and dam reservoirs as result of heat gradient, pollutant dispersion, and thermal plumes are some cases of non-homogeneous (i.e. variable density) gravity stratified flow fields [1]. Since most flows in nature and industry are almost always turbulent, and buoyancy has an important role in production and dissipation of turbulent kinetic energy, the accuracy of numerical simulation of turbulent buoyant flows is largely dependent on how well the buoyancy effects in turbulence are considered and modeled [2], [3].

Because of complexity of turbulence phenomenon and its modeling, turbulence has been the subject of diverse studies in different fields of engineering and science. Many turbulence models for different purposes and applicability have been proposed ranging from zero and one-equation models, the two-equation k-ε, k-ω and k-kl Mellor and Yamada model [4], Reynolds Stress Model (RSM), algebraic Stress Model (ASM) to more recent ones such as the Large Eddy Simulation (LES) and Direct Numerical Simulation (DNS) models. However, DNS and LES are less practical because of difficulty in numerical simulations, especially in complex flows, and the vast required computer resources [5].

Among the turbulence models, the Boussinesq based two-equation models have been able to satisfy engineering needs proportional to an acceptable accuracy [2], [3], [5]. In particular, the *k-ε* turbulence model is possibly the most extensively used because of its almost simplicity, stability in numerical methods, and less computing capacity, comparing to other complex models such as RSM and ASM or DNS and LES [3], [5]. However, the standard *k-ε* model with buoyancy terms needs especial modification to improve the prediction and consideration of buoyancy effects on production and destruction of turbulence in different turbulent buoyant flows [3], [5]–[7].

ASM and RSM use specific algebraic or partial differential equations to solve each individual Reynolds stress; therefore, ASM and RSM will be able to account for the buoyancy effects automatically and more realistically [5], [8]. However, they demand much more computational time and consequently are more costly. Beside the numerical difficulty, the model might suffer from a higher risk of instability in complex flow conditions [5]. Initial turbulence model developments utilized the Standard Boussinesq Gradient Diffusion Hypothesis (SGDH) to represent buoyancy induced turbulence generation. The mean deficiency of these models, like the *k-ε* model, is the isotropic eddy viscosity assumption, which does not take into account the non-isotropic behavior of turbulence due to buoyancy forces [7], [9], [10]. Moreover, in simulation of each specific turbulent buoyant flow, a suitable level of turbulent mixing with calibrated values for coefficients, as well as appropriate production and destruction terms are required; for example, in thermal simulations, the standard buoyancy modified *k-ε* model tends to under-predict the spreading rate of vertical buoyant plumes, and over-predict the spreading rate of horizontal, stably-stratified flows [5], [11], [12].

As RSM and ASM turbulence models solve transport equations for individual $\overline{u_i'u_j'}$ stress and $\overline{u_i'\phi'}$ flux components, they are able to take direct account of transport and history effects on these components and also of the anisotropy of the turbulent transport in complex flows; moreover, they

A.M. Bahari, Graduate student, K.N.Toosi University of Technology, Civil Engineering Department, P.O.Box:15875-4416, Tehran, Iran (corresponding author phone: +98-912-5104812; e-mail: mbahari@ sina.kntu.ac.ir).

K. Hejazi, Faculty of Civil Engineering Department, K.N.Toosi University of Technology, P.O.Box:15875-4416, Tehran, Iran (e-mail: hejazik@kntu.ac.ir).

introduce terms accounting for the effect of buoyancy automatically [8]. Therefore, the main attempts of previous researchers, related to buoyancy effects, have been to modify the simple two equation *k-ε* model on the basis of employing some relations from ASM or RSM models to consider direct effect of buoyancy on turbulence components. Thus, the relations for Reynolds stresses and turbulent scalar fluxes have been modified by this consideration. Daly and Harlow [13] proposed general gradient diffusion hypothesis (GGDH) for accounting turbulent scalar fluxes. Yan and Holmstedt [5] and Worthy et al. [6] in their studies on thermal plumes found that generalized diffusion hypothesis gives more realistic results. Davidson [9] combined ASM and *k-ε* formulas for Reynolds stress, and proposed a second closure correction method for accounting Reynolds stress components. Bonnet et al. [10] and Kun et al. [7] used this hybrid model in their studies respectively on coastal circulations modeling and vertical planar buoyant jets and came to more realistic results.

In this study we have implemented different considerations of computing turbulent scalar (e.g. salinity) fluxes and Reynolds stresses (i.e. turbulent stresses or turbulent momentum fluxes) in terms *P* and *G* in the *k-ε* equations on the basis of general gradient diffusion hypothesis of Daly and Harlow [13] for turbulent scalar fluxes and hybrid expression of Davidson [9] for Reynolds stresses. Along with these implementations, Henkes's [14] suggestion for controversial empirical constant, $c_{3\varepsilon}$, in ε equation has been used with a variable turbulent Schmidt number. To investigate the applicability of these solutions for gravity currents the experimental study of Gerber [15] on a horizontal saline gravity current has been simulated numerically and results have been compared to explore the most suitable turbulence model.

II. Buoyant $k-\varepsilon$ Models

A. The Standard k-ε Model with Buoyancy Terms

The standard buoyancy-modified *k-ε* model is based on the eddy- viscosity/diffusivity concept of Boussinesq, which uses an isotropic eddy-viscosity/diffusivity to relate the Reynolds stresses $\overline{u_i'u_j'}$ and turbulent flux $\overline{u_i'\phi'}$ of concentration or heat to the mean fields:

$$-\overline{u_i'u_j'} = \nu_t\left(\frac{\partial U_i}{\partial x_j}+\frac{\partial U_j}{\partial x_i}\right)-\frac{2}{3}k\delta_{i,j} \tag{1}$$

$$\overline{u_i'\phi'} = -\Gamma\frac{\partial \phi}{\partial x_i} = -\frac{\nu_t}{\sigma_t}\frac{\partial \phi}{\partial x_i} \tag{2}$$

where U_i and u_i' are respectively the mean and fluctuating velocity components in x_i direction, φ and φ' are the mean and fluctuating of either temperature or concentration (e.g., of salinity), ν_t is the turbulent or eddy viscosity, Γ is turbulent diffusivity of heat or concentration, and σ_t is the turbulent Schmidt number which relates eddy viscosity to the eddy diffusivity and its value can be an indication of the level of turbulent mixing. The production and dissipation of turbulent kinetic energy is subject to transport process, thus to describe the evolution of turbulence, two transport equations for *k* and *ε* are written in tensorial form as follows:

$$\frac{\partial k}{\partial t}+U_i\frac{\partial k}{\partial x_i} = \frac{\partial}{\partial x_i}\left(\frac{\nu_t}{\sigma_k}\frac{\partial k}{\partial x_i}\right)+P+G-\varepsilon \tag{3}$$

$$\frac{\partial \varepsilon}{\partial t}+U_i\frac{\partial \varepsilon}{\partial x_i} = \frac{\partial}{\partial x_i}\left(\frac{\nu_t}{\sigma_\varepsilon}\frac{\partial \varepsilon}{\partial x_i}\right)+ c_{1\varepsilon}\frac{\varepsilon}{k}(P+G)(1+c_{3\varepsilon}R_f)-c_{2\varepsilon}\frac{\varepsilon^2}{k} \tag{4}$$

where *P* represents the production of *k* by interaction of Reynolds stresses and mean-velocity gradient, and *G* represents the production/destruction of turbulence by buoyancy [16]:

$$P = -\overline{u_i'u_j'}\left(\frac{\partial U_i}{\partial x_j}\right) = \nu_t\left(\frac{\partial U_i}{\partial x_j}+\frac{\partial U_j}{\partial x_i}\right)\frac{\partial U_i}{\partial x_j} \tag{5}$$

$$G = -\beta g_i\overline{u_i'\phi'} = \beta g_i\frac{\nu_t}{\sigma_t}\frac{\partial \phi}{\partial x_i} \tag{6}$$

In the *k-ε* model the eddy viscosity ν_t, relates to *k* and *ε* via (7), which is obtained from a dimensional analysis and eddy viscosity concept [8].

$$\nu_t = c_\mu\frac{k^2}{\varepsilon} \tag{7}$$

In above equations $c_{1\varepsilon}$, $c_{2\varepsilon}$, $c_{3\varepsilon}$, β, and c_μ are empirical constants, g_i acceleration in x_i direction, and R_f is flux Richardson number. The R_f term is the ratio of the buoyancy production or dissipation of *k* to its production by the shear, $R_f = -G/P$ [16]. By this definition of R_f, in accordance with Rodi's argument [16], $c_{3\varepsilon}$ should be close to unity for vertical buoyant shear layers and close to zero for horizontal layers. To simplify this difficulty Rodi suggested an alternative definition of R_f, as $R_f = -G/(G+P)$. By this definition of R_f, miscellaneous value of $c_{3\varepsilon}$ has been proposed as optimized amounts. Another approach for $c_{3\varepsilon}$ is the suggestion of Henkes et al. [14] as follows:

$$c_{3\varepsilon} = \tanh\left|v/u\right| \tag{8}$$

Equation (8) expresses that in vertical shear layers and unstable stratifications which lateral component of velocity (v) has much greater value than horizontal component (u), the value of $c_{3\varepsilon}$ is close to unity, and in contrary, in horizontal shear layers it adopts a value almost equal to zero; therefore, the contribution ratio of buoyancy in turbulence is adjusted automatically.

For the other empirical constants the following standard values are specified [16]:

$$c_\mu = 0.09,\ c_{1\varepsilon} = 1.4,\ c_{2\varepsilon} = 1.92,\ \sigma_k = 1.0,\ \sigma_\varepsilon = 1.3 \qquad (9)$$

The turbulent transport is inversely proportional to the Schmidt number σ_t; its value, according to Rodi [16], is about 0.90 in near-wall flows, 0.50 in plane jets and mixing layers, and 0.70 in round jets. However, as σ_t can directly affect the level of turbulence, and buoyancy is one of the production/dissipation source terms of turbulence, its value should be modified by the effect of buoyancy force. One relation to account for this is the Munk-Anderson formula [16] as follows:

$$\sigma_t / \sigma_{t_0} = \frac{(1+3.33Ri)^{1.5}}{(1+10Ri)^{0.5}} \qquad (10)$$

$$Ri = -\frac{g}{\rho}\frac{\partial\rho/\partial z}{(\partial u/\partial z)^2} \qquad (11)$$

ρ is the density and Ri is the gradient Richardson number which is the ratio of gravity to internal forces and characterizes the importance of buoyancy effects. One may be able to fit definite experimental data by simply adjusting the constant σ_t as has been demonstrated by Gerber [15], and Nam and Bill [17], although, this may seems to vanished the generality of turbulence model [5]. In this paper $\sigma_t = 0.90$ has been used and is updated in each time step by (10).

B. The $k-\varepsilon$ Model with General Gradient Diffusion

The term G in k and ε equations represents an exchange between the turbulent kinetic energy and potential energy. In stable stratification it is negative and acts as a sink term which damps turbulence, while it is positive in unstable flows and acts as a source term that amplifies turbulence [16]. Thus, it can be understood that there is a direct relation between intensity of production/dissipation of turbulence by buoyancy and shear layer situation; it means that the greater stable stratification, the less turbulence production. It implies that in accounting for term G the direct effects of Reynolds stresses should be considered on prediction of turbulent scalar fluxes. A particular advantage of ASM is that terms accounting for buoyancy effect are in close correlation with turbulent stresses, so as an alternative to the standard gradient diffusion hypothesis of Boussinesq in accounting term G, the ASM relation of turbulent scalar fluxes (Φ) can be used as follows:

$$\overline{u_i'\Phi'} = \frac{k}{c_1\varepsilon}\left(-\overline{u_i'u_j'}\frac{\partial\Phi}{\partial x_j} - (1-c_2)\overline{u_j'\Phi'}\frac{\partial U_i}{\partial x_j} - (1-c_3)\beta a_{gi}\overline{\Phi'^2}\right) \qquad (12)$$

where $\overline{\Phi'^2} = -2R(k/\varepsilon).\overline{u_i'\Phi'}.\partial\Phi/\partial x_i$, and c_1, c_2, c_3, and R are constants [8].

Shabbir and Taulbee [12] in their study on buoyant plumes found that the magnitude of G predicted by (12) agrees well with measured data, while it is likely to be under-estimated, using standard gradient diffusion hypothesis. Yan and Holmestedt [5] tried to implement above expression to compute turbulent scalar (i.e. heat) flux in their study; however, they encountered problem to reach convergence. Daly and Harlow [13] proposed the so-called generalized gradient diffusion hypothesis, which is simpler than above ASM formula but retains its basic features:

$$\overline{u_i'\phi'} = -\tfrac{3}{2}\frac{c_\mu}{\sigma_t}\frac{k}{\varepsilon}\overline{u_i'u_j'}\frac{\partial\phi}{\partial x_j} \qquad (13)$$

using above expression, the term G becomes:

$$G = \beta g_i \tfrac{3}{2}\frac{c_\mu}{\sigma_t}\frac{k}{\varepsilon}\overline{u_i'u_j'}\frac{\partial\phi}{\partial x_i} \qquad (14)$$

Therefore, according to this and recommendations of Gerber [15] in his experimental study of same field of interest, saline gravity current, We used (14) in accounting for term G in the second turbulence closure.

C. The k-ε Model with Davidson's Second-order Correction for Term P.

A particular limitation of turbulence models based on the eddy-viscosity/diffusivity concept, concerning buoyant flows, is that they cannot describe non-isotropic behavior of turbulence. This non-isotropy which is due to Buoyancy force or Earth rotation in geophysical flows is characterized by amplification of the turbulent fluctuations in one direction and damping it in the other one [10]. Second-order closure schemes which employ transport equations for each $\overline{u_i'u_j'}$ and $\overline{u_i'\phi'}$ components have been developed to hinder this deficiency. However, these models like RSM and ASM give complex relations which need large amount of time and cost for practical use. In ASM turbulent stresses are computed through (15) [5], [7], [8]:

$$\overline{u_i'u_j'} = \frac{2}{3}\delta_{ij}k + \frac{k}{\varepsilon}\frac{(1-c_2)(P_{ij}-2/3\,\delta_{ij}P)}{c_1+(P+G)/\varepsilon-1} + \frac{k}{\varepsilon}\frac{(1-c_3)(G_{ij}-2/3\,\delta_{ij}G)}{c_1+(P+G)/\varepsilon-1} \qquad (15)$$

where

$$P_{ij} = -\overline{u_i'u_l'}\frac{\partial U_i}{\partial x_l} - \overline{u_j'u_l'}\frac{\partial U_i}{\partial x_l} \qquad (16)$$

$$G_{ij} = -\beta\overline{u_i'\phi'}g_j - \beta\overline{u_j'\phi'}g_i \qquad (17)$$

Davidson [9] proposed a second closure correction method to simplify above relation while it preserves its advantages. In this method Reynolds stresses consist of two parts: the non-isotropic turbulence stresses due to buoyancy force and isotropic turbulence part due to shear production; the first part will be calculated through ASM model and the second part is

as given by standard *k-ε* model on the basis of Boussinesq assumption, that is:

$$\overline{u_i'u_j'} = (\overline{u_i'u_j'})_{ASM} + (\overline{u_i'u_j'})_{k-\varepsilon} \tag{18}$$

where

$$(\overline{u_i'u_j'})_{ASM} = \frac{k}{\varepsilon}\frac{(1-c_3)(G_{ij}-2/3\,\delta_{ij}G)}{c_1+(P+G)/\varepsilon-1} \tag{19}$$

$$(\overline{u_i'u_j'})_{k-\varepsilon} = -\nu_t\left(\frac{\partial U_i}{\partial x_j}+\frac{\partial U_j}{\partial x_i}\right)-\frac{2}{3}k\delta_{i,j} \tag{20}$$

$$G_{ij} = -\beta\overline{u_i'\phi'}g_j - \beta\overline{u_j'\phi'}g_i \tag{21}$$

therefore the total production term, *P* becomes:

$$P = P_{ASM} + P_{k-\varepsilon} = -\left(\frac{k}{\varepsilon}\frac{(1-c_3)(G_{ij}-2/3\,\delta_{ij}G)}{c_1+(P+G)/\varepsilon-1}\right)\frac{\partial U_i}{\partial x_j} + \nu_t\left(\frac{\partial U_i}{\partial x_j}+\frac{\partial U_j}{\partial x_i}\right)\frac{\partial U_i}{\partial x_j} \tag{22}$$

Equation (18) can also be used for accounting term *G* in (14); however, Yan and Holmestedt [5] found that utilizing this equation simultaneously for both *G* and *P* can cause numerical difficulty. In the present study this relation has only been used for term *P*. Regarding local equilibrium assumption according to the Rodi [16], the term "*(P+G)/ε–1*" in (22) will be omitted; Rodi demonstrated that equilibrium assumption does not affect the accuracy of the ASM model. We have used this assumption herein.

III. Numerical Modeling

An arbitrary Lagrangian-Eulerian (ALE) 2D vertical hydrodynamic numerical model has been deployed, based on time dependent Reynolds-averaged Navier-Stokes equations to simulate saline gravity currents. The model is further refined and developed for different *k-ε* turbulence closures. A structured non-orthogonal curvilinear staggered mesh is used for computational domain. To discrete flow and transport equations of velocities and scalar quantities like salinity, concentration, *k* and *ε*, finite volume method was utilized, providing flexibility for defining control volumes in a staggered grid system, especially near the bed and water surface, where rapid changes of bathymetry and free surface may have significant effect on the prediction of the flow flied. Moreover, the finite volume method provides the assurance of global conservation.

A. Governing Equations in ALE

In the ALE method the mesh motion can be chosen arbitrarily; the newly updated free surface is determined purely by Lagrangian method, by the velocity of fluid particles at the free surface. Therefore, in horizontal direction the grids are fixed while they move in vertical direction. The grid geometry is computed and redistributed after completion of each time step. With this consideration, an additional grid velocity w_g, appears in the the Navier-Stokes and species concentration equations. The set of equations of continuity, momentum and species concentration (*C*) in two directions is written as follows:

$$\frac{\partial u}{\partial x}+\frac{\partial w}{\partial z}=0 \tag{23}$$

$$\frac{\partial u}{\partial t}+\frac{\partial u^2}{\partial x}+\frac{\partial uw}{\partial z}-w_g\frac{\partial u}{\partial z}=-\frac{1}{\rho_r}\frac{\partial p}{\partial x}+\frac{\partial}{\partial x}\left((\nu_t+\nu)\frac{\partial u}{\partial x}\right)+\frac{\partial}{\partial z}\left((\nu_t+\nu)\frac{\partial u}{\partial z}\right) \tag{24}$$

$$\frac{\partial w}{\partial t}+\frac{\partial wu}{\partial x}+\frac{\partial w^2}{\partial z}-w_g\frac{\partial w}{\partial z}=-\frac{1}{\rho_r}\frac{\partial p}{\partial z}+\frac{\partial}{\partial x}\left((\nu_t+\nu)\frac{\partial w}{\partial x}\right)+\frac{\partial}{\partial z}\left((\nu_t+\nu)\frac{\partial w}{\partial z}\right)-g\frac{\rho-\rho_r}{\rho_r} \tag{25}$$

$$\frac{\partial C}{\partial t}+\frac{\partial uC}{\partial x}+\frac{\partial wC}{\partial z}-w_g\frac{\partial C}{\partial z}=\frac{\partial}{\partial x}\left((\nu_t+\nu)\frac{\partial C}{\partial x}\right)+\frac{\partial}{\partial z}\left((\nu_t+\nu)\frac{\partial C}{\partial z}\right) \tag{26}$$

where *u* and *w* are velocity components in *x* and *z* directions respectively, *ρ* is the local density and ρ_r a reference density, *v* is kinematic viscosity, and *g* is the gravitational acceleration.

B. Solution Method

The projection (fractional-step) method, proposed by Chorin [18] and Temam [19], has been adopted. The method generally is accomplished in two steps; the pressure gradient terms are omitted from the momentum equations in the first step. The transport part of Navier-Stokes equations including advection and diffusion are advanced in time to obtain a provisional velocity field U^*. In the second step, the provisional velocity is corrected by accounting for the pressure gradient and continuity equation as follows:

$$\frac{U^{n+1}-U^*}{\Delta t}+\nabla P^{n+1}=0 \tag{27}$$

Subject to the continuity constraint:

$$divU^{n+1}=0 \tag{28}$$

by taking the divergence of (27), the continuity equation will be exerted and the Possion equation is obtained:

$$\nabla^2 P^{n+1}=\frac{divU^*}{\Delta t} \tag{29}$$

From the above equations the pressure distribution is obtained and velocity quantities are then updated. Advection

and diffusion parts of transport equations were computed in a locally one-dimensional manner in sub-sub-fractional-steps in two directions. A fifth degree accurate scheme for advection and the Crank-Nicolson method has been utilized for diffusion computations.

C. k-ε Numerical Models

According to (3) and (4) the *k-ε* equations consist of a transport part and source terms including *P* and *G* variables. Although transport part of equations is commonly used in existing turbulence closures *k-ε* models, the term *P* and *G* have been used differently in a variety of research in this area. The transport equations for *k* and *ε* have been solved by fractional step method. In the first fractional time step the values have been advected in sub-fractional steps for each direction and in the second fractional time step the values have been diffused in *x* and *z* directions in the same manner. Discrete equations for *k* and *ε* in ALE form are as follows:

k-equation:

$$\frac{k^{n+1}-k^{n}}{\Delta t}+\frac{\partial}{\partial x}\left(u^{n}\ k^{n}\right)+\frac{\partial}{\partial z}\left(w^{n}\ k^{n\xrightarrow{A_x}n+1}\right)-$$
$$w_g^{n}\ \frac{\partial}{\partial z}\left(k^{n\xrightarrow{A}n+1}\right)=$$
$$\frac{\partial}{\partial x}\left[\frac{\nu_T^{n}}{\sigma_k}\frac{\partial}{\partial x}\left((1-\theta)\,k^{n\xrightarrow{A}n+1}+\theta\,k^{n\xrightarrow{D_x}n+1}\right)\right]+$$
$$\frac{1}{2}\frac{\partial}{\partial z}\left[\frac{\nu_T^{n}}{\sigma_k}\frac{\partial}{\partial z}\left((1-\theta)\,k^{n\xrightarrow{D_x}n+1}+\theta\,k^{n\xrightarrow{D}n+1}\right)\right]$$
$$+P^{n}+G^{n}-\frac{1}{2}\left(\frac{\varepsilon}{k}\right)^{n}\left(k^{n\xrightarrow{D_x}n+1}+k^{n\xrightarrow{D}n+1}\right) \tag{30}$$

ε-equation:

$$\frac{\varepsilon^{n+1}-\varepsilon^{n}}{\Delta t}+\frac{\partial}{\partial x}\left(u^{n}\ \varepsilon^{n}\right)+\frac{\partial}{\partial z}\left(w^{n}\ \varepsilon^{n\xrightarrow{A_x}n+1}\right)-$$
$$w_g^{n}\ \frac{\partial}{\partial z}\left(\varepsilon^{n\xrightarrow{A}n+1}\right)=$$
$$\frac{\partial}{\partial x}\left[\frac{\nu_T^{n}}{\sigma_\varepsilon}\frac{\partial}{\partial x}\left((1-\theta)\,\varepsilon^{n\xrightarrow{A}n+1}+\theta\,\varepsilon^{n\xrightarrow{D_x}n+1}\right)\right]+$$
$$\frac{\partial}{\partial z}\left[\frac{\nu_T^{n}}{\sigma_\varepsilon}\frac{\partial}{\partial z}\left((1-\theta)\,\varepsilon^{n\xrightarrow{D_x}n+1}+\theta\,\varepsilon^{n\xrightarrow{D}n+1}\right)\right]$$
$$+c_{1\varepsilon}\left(\frac{\varepsilon}{k}\right)^{n}\left(P^{n}+c_{3\varepsilon}\,G^{n}\right)-$$
$$c_{2\varepsilon}\,\frac{1}{2}\left(\frac{\varepsilon}{k}\right)^{n}\left(\varepsilon^{n\xrightarrow{D_x}n+1}+\varepsilon^{n\xrightarrow{D}n+1}\right) \tag{31}$$

Therefore the viscosity is obtained:

$$\nu_T^{n+1}=c_\mu\left(\frac{k^2}{\varepsilon}\right)^{n+1} \tag{32}$$

In the above equations "→" indicates the sub fractional time that a specific process has been performed; these processes have been indicated by:

A_x: Advection in x-direction has been completed.

A: Advection in both directions has been completed.

D_x: Diffusion in x-direction has been completed.

D: Diffusion in both directions has been completed.

D. Simulation of a Gravity Current

To investigate the alternate *k-ε* models in buoyant flow fields, the gravity current studied experimentally by Gerber [15] has been simulated. The experiment was carried out in a Perspex flume with an inlet for the salt current with an excess density of 2 kg/m^3 with respect to water, and flux of 0.59 l/s. The gravity current was planned to travel along the flume bottom and exit it to a damping tank to prevent creation of a reverse flow to the upstream. The detail of experimental apparatus is elaborated in Fig. 1.

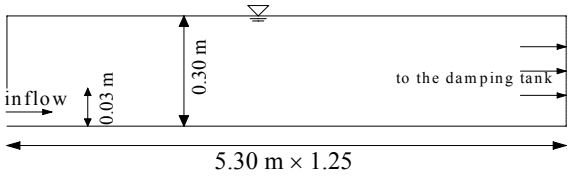

Fig. 1 Experimental flume

General characteristics of flow and inlet conditions which is utilized in laboratory experiment by Gerber [15] and the simulations are summarized in Table I.

TABLE I
SUMMARY OF INLET FLOW CONDITIONS

Parameter	Units	Value
water depth in flume	m	0.30
depth of inlet current	m	0.03
ambient density	kg/m^3	9982
excess fractional density	kg/m^3	2.0
inlet velocity	m/s	0.079
k_0	m^2.s^{-2}	6.875×10^{-5}
ε_0	m^2.s^{-3}	1.38×10^{-5}

The boundary at the inlet is as has been tabulated in Table I and illustrated in Fig. 1. At the free surface no flux conditions are imposed. At the bottom, (33) and (34) are applied to estimate the turbulence kinetic energy and its dissipation next to the bed [16], [19]:

$$k=\frac{u_*^2}{\sqrt{c_\mu}} \tag{33}$$

$$\varepsilon=\frac{u_*^3}{\kappa.z_0} \tag{34}$$

where u_* is shear velocity, κ is the von Karman constant with a value of 0.41[20], and z_0 denotes the roughness height.

IV. Results and Discussion

Four alternatives of the k-ε turbulence model which are applied in simulation of the gravity current are summarized as follows:

Model No.1: The standard k-ε model with buoyancy terms, and a variable buoyancy coefficient $c_{3\varepsilon}$ and Schmidt number according to (8) and (10).

Model No.2: The standard k-ε model with buoyancy terms, and using general gradient diffusion hypothesis for accounting turbulent scalar flux in term G according to (14).

Model No.3: The standard k-ε model with buoyancy terms, which term P is modeled on the basis of second-order correction of Davidson [9] which combines the standard k-ε model and algebraic stress model (ASM) according to (22).

Model No.4: The standard k-ε model with buoyancy terms which term P is calculated by Davidson second-order correction method, and G by general diffusion hypothesis according to (14) and (22) respectively.

The time series of simulated saline gravity current of models No.1 and No.2 have been shown in Figs. 2 and 3; contours show the amount of salinity within the current. Model No.2 shows approximately a higher spreading rate than model No.1; but, the propagation speed of the gravity current front in model No.2 is lower than model No.1, which has led to a shorter traveled distance.

Tables II and III represent the maximum values of the gravity current thickness and velocity of the gravity current front predicted by different models as well as experimental results for two points in the flume. In addition, the results of Fluent package which are stimulated by Gerber [15] is reported herein. Fig. 4 reports the estimated eddy viscosity value by each turbulence model.

The simulation results of maximum velocity of the front and current thickness show good correlation with the computed ranges of eddy viscosity; the greater the turbulence intensity, the greater the gravity current thickness and the less the maximum velocity. Moreover, as eddy viscosity increases, the model is more diffusive and consequently more turbulent mixing and spreading rate is predicted which leads to a higher gravity current height.

Differences in the estimated values and closeness to the experimental measurements provide the level of the efficiency of each model in horizontal gravity current simulation. To compare the four simulations, model No.2 and No.4 have lower velocity and higher current thickness. Model No.1 has a closer prediction compared to measured values. While model No.3 does not show any considerable improvement over model No.1, it shows more realistic predictions than model No.2 and No. 4. Comparing the results of numerical simulation and measured values in Table II and Table III in conjunction with Fig. 4, the accuracy of the model decreases as the level of prediction of intensity of turbulence increases. Therefore, in a horizontal gravity current simulation a turbulence model with a lower level of mixing intensity may be more applicable, and this may demonstrate the reason that for two different Schmidt numbers, used in Fluent simulation by Gerber [15], the higher value gives the more accurate results.

Model No.2 and No. 4 which utilize the general gradient diffusion hypothesis give higher turbulence intensity and accordingly are less accurate.

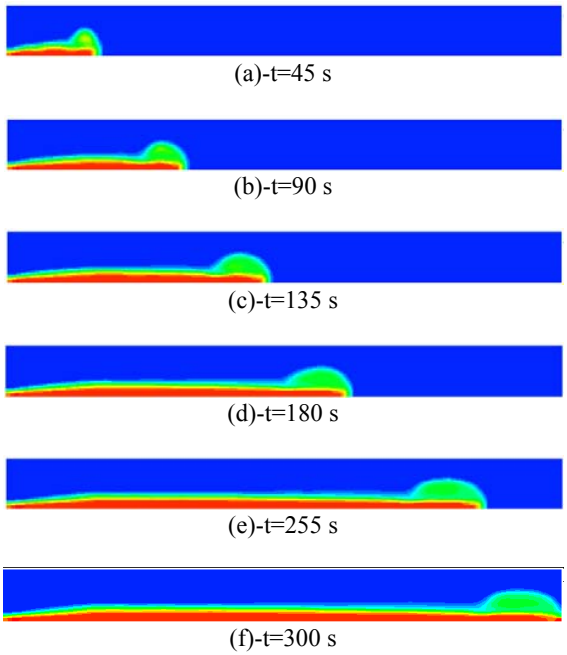

Fig. 2 Time series of gravity current, Model No.1

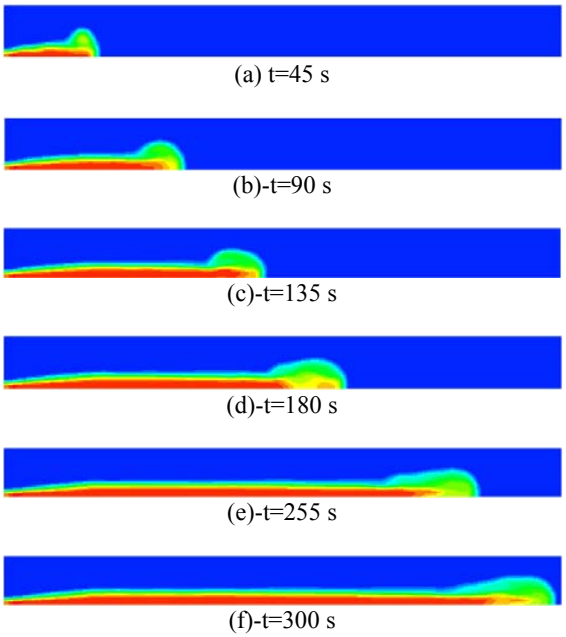

Fig. 3 Time series of gravity current, Model No.2

TABLE II
FLOW PARAMETERS FOR X = 0.9 FROM INLET

Test case	U_{max}(m/s)	H_d(m)
measured values	0.0620	0.070
model No.1	0.0563	0.095
model No.2	0.0544	0.102
model No.3	0.0560	0.098
model No.4	0.0540	0.105
fluent (σ_t = 0.7)	0.0409	-
fluent (σ_t = 1.3)	0.0450	-

H_d = density current height

TABLE III
FLOW PARAMETERS FOR X = 2.4 FROM INLET

Test case	U_{max}(m/s)	H_d(m)
measured values	0.0487	0.124
model No.1	0.0453	0.127
model No.2	0.0441	0.131
model No.3	0.0450	0.129
model No.4	0.0439	0.131
fluent (σ_t = 0.7)	0.0325	-
fluent (σ_t = 1.3)	0.0342	-

H_d = density current height

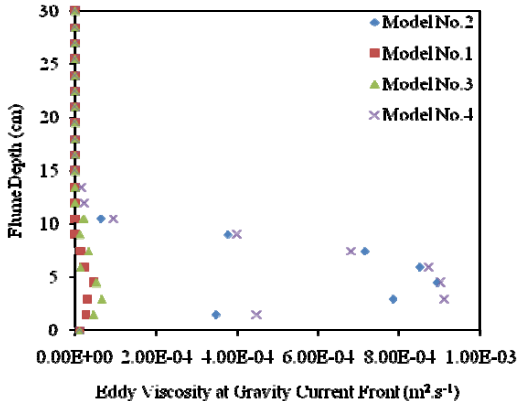

Fig.4 Predicted Eddy viscosity by different models

Model No.3 makes very little change in increasing turbulence intensity compared to model No.1, and similarly, Model No.4 shows slightly higher turbulence intensity compared to Model No.2. Therefore, the slight higher intensity of turbulence caused by (19) is not regarded as an advantage of using ASM relation in a horizontal density current. However, in contrary to ASM model, this equation does not increase computational time and may propose advantages for other flows situation where turbulent motion and mixing are more dominant.

Concerning the turbulence structure at the head and body of the current, simulations show that turbulence is proportional to dense current height which is in consistence to Kneller et al. [20], that the dominant length scale of turbulent eddies is nearly equal to thickness of gravity current. Moreover, the turbulence (eddy viscosity) reaches its maximum value at the current head where the large eddies are generated and gravity current has its maximum thickness.

V. CONCLUSION

A gravity wall jet was simulated to investigate the buoyancy effects in four different *k-ε* turbulence models. Basically, the gravity wall jet seems to be largely inclined to a stable stratified situation, in which buoyancy damps the turbulence and therefore the contribution of G in turbulence production is less. General gradient diffusion hypothesis predicts a higher value of eddy viscosity at the current head and consequently a greater spreading rate. Using Davidson [9] second-order correction shows a slight increase of eddy viscosity either in combination with general gradient hypothesis (model No.4) or without it (model No.3). Regarding the over-estimated values of simulations, it is recommended that the influence of general gradient diffusion hypothesis and hybrid relation of Davidson [9] to be investigated for a flow domain that turbulent mixing is more governing and shear layers have mainly unstable arrangement, which buoyancy magnifies the turbulence production.

By increasing in the eddy viscosity (turbulence intensity), the depth of gravity current grows and propagation speed decreases, hence a shorter traveled distance for current is predicted.

The simulation with turbulence closure No.1 which applies a variable $c_{3\varepsilon}$ and Schmidt number gives the best result, comparing to the other models and Fluent simulation; therefore, it is very important to consider an appropriate Schmidt number as well as $c_{3\varepsilon}$, if a variable value is not used.

Results show that both general gradient diffusion (14) and Boussinesq (7) expressions for turbulent scalar fluxes over predict the spreading rate in this specific simulation, and since the spreading rate can be an indicator of the level of turbulence [15], it seems that lower turbulence intensity closures would be more suitable. Finally, concerning the use of general gradient diffusion hypothesis for term *G* and second-order correction of term *P*, although in this certain simulation they led to greater turbulent kinetic energy production, further researches on different turbulent buoyant flows are needed to come to definite conclusion about their applicability in each especial problem. It is also worth noting that a distinct turbulence model and especially *k-ε* model cannot satisfactory predict all turbulent flow cases, and especial calibration for constants and consideration for source terms are needed.

REFERENCES

[1] Simpson, J., "Gravity Currents in the Environment and the laboratory," *Cambridge University Press,* 1997.
[2] Wilcox, D. C., "Turbulence modeling for CFD, Third Edition," Birmingham Press, Inc., San Diego, California, 2006.
[3] Nicolette, V.F., Tieszen, S. R., Black, A. R., Domino, S. P., O'Hern, T. J., "A Turbulence Model for Buoyant Flows Based on Vorticity Generation," Sandia National Laboratory, Sandia Report, SAND2005-6273, 2005.
[4] Mellor, G. L., Yamada, T., "Development of Turbulence Closure Model for Geophysical Fluid Problems," *Reviews of Geophysics and Space Physics, J.,* vol.20, No.5, 1982, pp. 851-875.

[5] Yan Z., Holmstedt G., "A two-equation model and its application to a buoyant diffusion flame," *International Journal of Heat and Mass Transfer,* vol.42, 1999, pp. 1305-1315.
[6] Worthy, J., Sanderson, V., and Rubini, P., "A Comparison of Modified k-ε Turbulence Models for Buoyant Plumes", Cranfield University Library, Staff Publications, School of Engineering, 2001.
[7] Kun, Y., Yiping, H., Xueyi, Z., Yuliang, L., "Study on Anisotropic Buoyant Turbulence Model," *Applied Mathematic s and Mechanics J.,* vol.21, No.1, 2000, pp. 43-48.
[8] Rodi, W., "Examples of Calculation Methods for Flow and Mixing in Stratified Fluids," *Geophysical Research J.,* vol.92, No.C5, 1987, pp. 5305-5328.
[9] Davidson L., "Second-order Correction of the k-ε Model to Account for Non-isotropic Effects due to Buoyancy," *International Journal of Heat and Mass Transfer,* vol.33, 1990, pp. 2599-2608.
[10] Verdier-Bonnet, C., Angot, Ph., Fraunie, Ph., Coantic, M., "Three Dimensional Modeling of Coastal Circulations with Different k-ε Closures," *Marine System J.,* vol.21, 1999, pp. 321-339.
[11] Annarumma, M.O., Most, J.M., Joulain, P., "On the Numerical Modeling of Buoyant-dominated Turbulent Vertical Diffusion Flames," *Combustion and Flame J.,* vol.85, 1991, pp. 403-415.
[12] Shabbir, A., Taulbee, D. B., "Evaluation of Turbulence Models for Predicting Buoyant Flows," *Heat Transfer J.,* vol. 112, 1990, pp. 945-951.
[13] Daly B. J., Harlow F. H., Transport equations of turbulence, *Journal of Physics Fluids,* Vol. 13, 1970, pp. 2634-649.
[14] Henkes, R.A.W.M., LeQuere, P., Three Dimensional Transition of Natural-Convection Flows, *Journal of Fluid Mechanics,* vol.319, 1996, pp. 281-303.
[15] Gerber, G. Experimental Measurement and Numerical Modeling of Velocity, Density and Turbulence Profiles of a Gravity Current, PhD Thesis, *University of Stellenbosch*, 2008.
[16] Rodi, W. "Turbulence Models and their Applications in Hydraulics" A State of the Arts Review, University of Karlsruhe, Germany, 1984.
[17] Nam, S., Bill, R.G., "Numerical Simulation of Thermal Plumes," *Fire Safety J.,* vol.21, 1993, pp. 231-256.
[18] Chorin, A.J., "Numerical Solution of the Navier-Stokes Equations," *Mathematics of Computation J.,* vol.22, 1968, pp. 745-762.
[19] Temam, R., "Sur l´Approximation de la Solution des Equation de Navier-Stokes par la Méthode des pas Fractionnaires," *Archive for Rational Mechanics and Analysis,* vol.32, 1969, pp. 135-153.
[20] Kneller, B. C., Bennet, S. J., McCaffrey, W. D., "Velocity Structure, Turbulence and Fluid Stresses in Experimental Gravity Currents," *Geophysical Research J.,* vol.104, No.C3, 1999, pp. 5381-5391.